TÉCNICO LISBOA

Control of Cyber-Physical System

Master Degree in Electrical and Computer Engineering

Lab Report 1

Authors:

Ayesha Aslam (1109220) ayesha.aslam@tecnico.ulisboa.pt
Farooq Olanrewaju (1109173) olanrewajufarooq@yahoo.com
Md Sazidur Rahman (1109170) md.sazidur.rahman@tecnico.ulisboa.pt

Group 11

2023/2024 – 1st Semester, P1

Contents

1 Introduction

The system consists of a vertically oriented motor with a flexible bar attached to it. A potentiometer is used in instrumentation to gauge the axis' angle. A strain gauge and a Wheatstone-Bridge are used in conjunction to determine the bar's deflection.
The two constants that define these two measuring systems are discovered during sensor calibration. The motor that drives the arm is then connected to the angular location of its tip using a model of the plant. This model will be employed for control design in the future.

2 Plant Description

2.1 Describe reasons that cause this control objective to be nontrivial.

The motor's speed is determined by the applied voltage rather than its position. Feedback is necessary to monitor the voltage over time. A constant voltage leads to a steady angular velocity. Since the motor shaft is positioned vertically, gravity's influence does not need to be considered in our laboratory experiment. Due to disruptions and inaccuracies in the model, it's highly unlikely to achieve the accurate position without any feedback, even when using consistent reference signals. In addition, overshooting is expected when providing an impulse as an input signal to the motor. Even if we assume that the motor is perfect, there will always be overshooting, and the bar will vibrate with little damping.
To make a guess on where the poles are, we split the system into smaller parts. We can estimate the motor by using an integrator, which means its pole should be at the origin of the s-plane. The second part of the system consists of the arm bending around the shaft. When excited, we can see that there is a complex conjugate pole pair in left plane of the s-plane. It is necessary to state that this system separation is possible after locating the poles roughly because the transfer functions are multiplied when two systems are connected in series. Because of this, the behavior of the entire system nevertheless exhibits the poles of the two subsystems. Because of this, the behavior of the entire system nevertheless exhibits the poles of the two subsystems.
The control objective is further complicated by the fact that the tip location cannot be directly measured. The ensuing section presents the countermeasures for this issue. Therefore, the control goal for this system is nontrivial.

3 Sensor Calibration

3.1 Comment on the motor operation.

The DC motor on the Rotary Servo Base Unit is used to rotate the flexible link from one end in the horizontal plane. The motor end of the link is instrumented with a strain gauge that can detect the deflection of the tip. The strain gauge outputs an analog signal proportional to the deflection of the link. The deflection angle of the link increases positively when rotated counter-clockwise. The servo angle,θ, increases positively when it rotates counter-clockwise (CCW). The servo turns in the CCW direction when the control voltage is positive.
The open-loop operation of a DC servo motor with a constant command signal results in an

inability to accurately control its angular position due to the absence of feedback and the presence of various factors that can affect motor behavior. Over time, drift, load variations, voltage fluctuations, and external disturbances can accumulate, causing the motor's angular position to never stabilize at the desired set-point.The motor can be viewed as an integrator because a constant voltage results in a constant change in angle. To achieve stable and precise angular position control with a DC servo motor, a closed-loop control system with feedback sensors is typically necessary to continuously monitor and correct any deviations from the desired position.

3.2 Explain the procedure carried out to perform sensor calibration.

In order to transmit signals to the motor, we designed a Simulink block diagram, as depicted in figure 1. This Simulink diagram includes a signal generator responsible for sending a predefined signal to the motor. The motor receives this signal via the analog output block, simultaneously recording it in the scope. To read data from the sensors, we integrated an analog input block to visualize the sensor signals. Given that our system involves two sensors, we incorporated two analog input blocks.

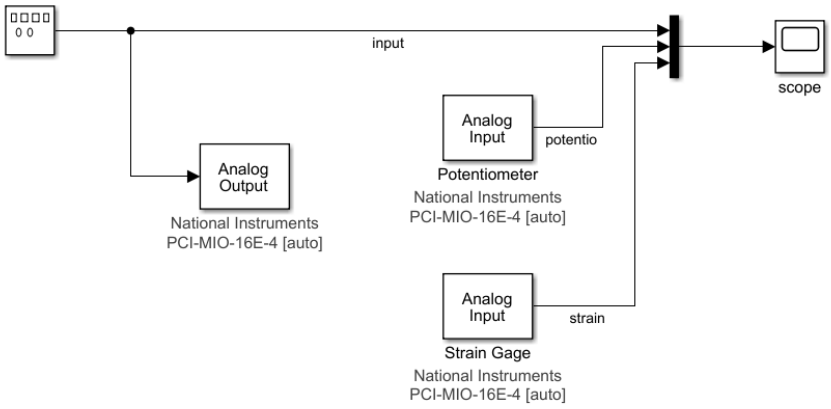

Figure 1: Simulink Block Diagram

3.2.1 Calibration of potentiometer sensor model:

The potentiometer is used to measure the shaft angle. A cursor connected to the motor shaft slides over a resistive wire, changing resistance proportionally to the angle. An electric circuit converts this resistance into an electrical voltage value. Therefore, the shaft angle θ is approximately given as a function of the sensor output θ_e by:

$$\theta = \theta_e K_p$$

where K_p is a constant with units [degree/V].

To obtain the Voltage (tensions) at different angles, we performed a set of experiments by manually moving the gear at different angles and recorded the output voltages. Table 1 below shows the shaft angle θ and the sensor output θ_e.

Table 1: Potentiometer readings

θ (degree)	θ_e (V)
0	1.9043
-45	0.7324
45	3.1787
22.5	2.5781
-22.5	1.4844

Gradient of the plot of voltage against angles as shown in figure 2b gives us the value of K_p.The value of $\mathbf{K_p}$ obtained from our experiment is $\mathbf{37.39deg/V}$.

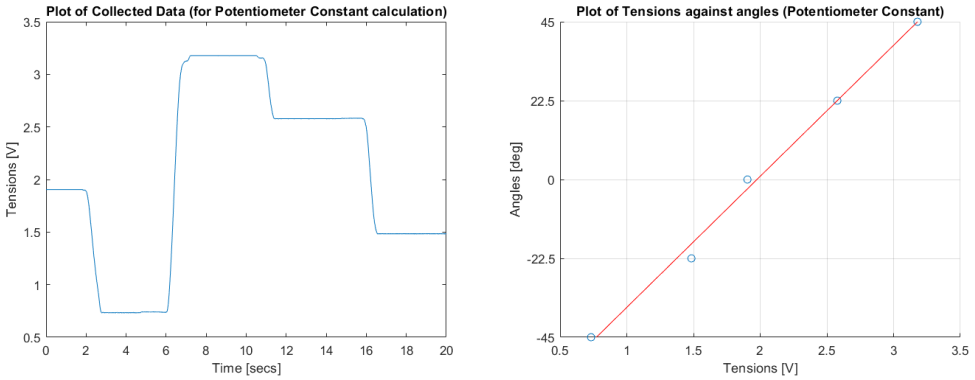

(a) Data obtained from potentiometer **(b)** Plot of tension against angles for K_p

3.2.2 Calibration of bar deflection model:

In order to estimate the value of the constant K_e, a sequence of experiments is done, each experiment consisting of deflecting the bar by a known quantity and reading the corresponding electrical tension. The bar is rigidly attached to a support stand. In the end of the stand there is a calibration "comb" with several slots separated by 1/4 inch (1 inch $= 2,54cm$) that allows to deflect the bar by known quantities. This constant is estimated from the set of data obtained in the different experiments using the least squares algorithm.In the case of the flexible bar, the sensor provides an electrical tension α_e that is related to the actual deflection angle α by:

$$\alpha = \alpha_e K_b$$

where K_b is a constant with units [degree/V].

Strain-gauge values for corresponding deflections is displayed in table 2.

Table 2: Strain-gauge readings

α (degree)	α_e (V)
6.2667	-0.7373
5.2436	-0.6006
4.2204	-0.4736
3.1973	-0.3418
2.1742	-0.2246
1.1510	-0.0928
0.1279	-0.0146
-0.8952	0.1514
-1.9184	0.3027
-2.9415	0.4297
-3.9647	0.5615
-4.9878	0.7031
-6.0109	0.8301
-7.0341	1.0010
-8.0572	1.0889

Gradient of the plot of tension against angles as shown in figure 3b gives us the value of K_b.The value of $\mathbf{K_b}$ obtained from our experiment is $\mathbf{-7.77 deg/V}$.

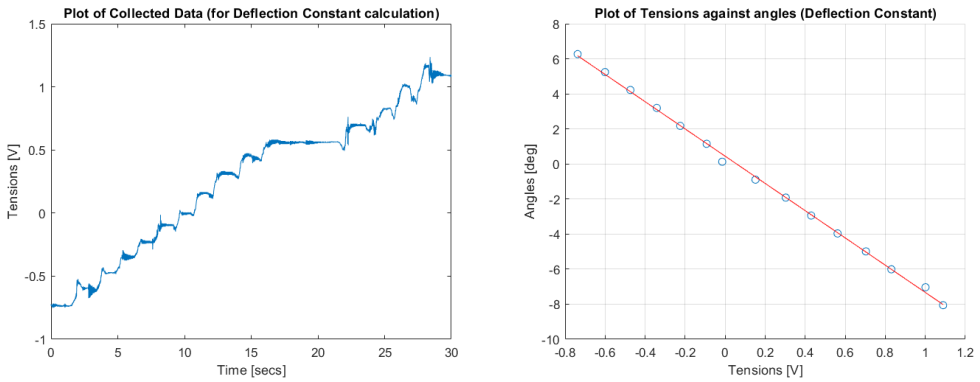

(a) Data obtained from strain-gauge **(b)** Plot of tension against angles for K_b

4 Plant Model Identification

4.1 Description of Experiment

To identify the plant model we started running several tests to collect data. We have taken data of different frequencies and amplitudes. The amplitude was square wave within the limit of $0.5V$ and $1.5V$ & the frequency was between $0.4Hz$ and $1.5Hz$.
Depending on the excitation signal given the bar would move faster or slower (depending on the frequency) and the range would vary depending on the amplitude given. As long as a square wave was given the bar moved regularly.

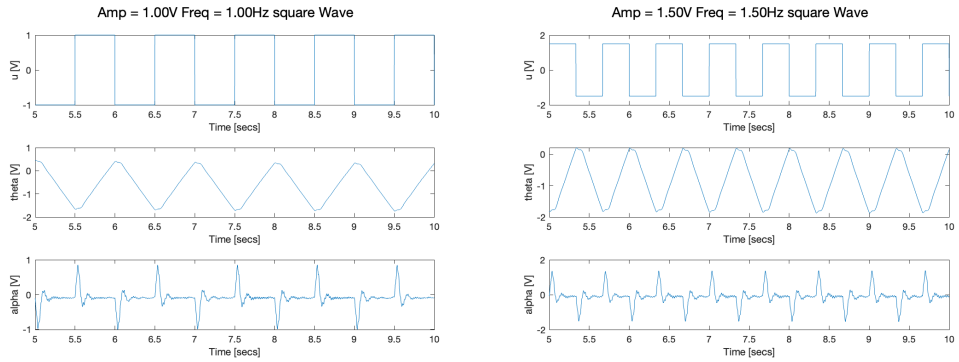

Figure 4: Influence of amplitude and frequency comparison

Figure 4 shows the comparison of the effect between amplitude and frequency. When the bar is moved, we can see that the effects of varied amplitude and frequency are very evident. On the basis of this, we were able to determine how the input's amplitude and frequency affect movement. In order to obtain the ideal data for our upcoming model, we started by creating a number of pseudo random binary signals (PRBS) with a sample time of 0.002 s.

4.2 Data Sampling Frequency

The sampling time needs to be carefully chosen in order to understand the dynamics of the model completely. The approximate frequency at which the plant will operate must first be estimated. Since the specific frequency depends on how the plant is excited, orders of magnitude will do for the time being. Given that we anticipate various harmonics in the output signal, the selected sampling rate should ensure that many samples are collected throughout each interval. Usually, the more samples, the better, but for this, having too many samples will cause noise and data differentiation to skew the identification. These can bring about undesirable behavior and harm parameter identification. A sampling frequency of $\frac{1}{0.002}hz$ is estimated to capture the dynamics.

4.3 Plant Identification Considerations

4.3.1 Effect of Data Filtering on Identification

After filtering the data for a variety of reasons, the model is identified: It is possible to carry out system identification without paying attention to the motor's integrating impact because of prior knowledge of its effect. As a result, the data collected during the testing are distinct. As a result, the system identity has a stronger connection to the bar subsystem while accounting for some less than optimal consequences of the motor without the integrator. Applying the differentiation implies that the identification needs to consider one less factor since this component is already known. Signals must be filtered due to measurement noise in order to produce data that more accurately reflects the nature of the system. It is well known that the system is slow because of the components' inertia. The usage of a low pass filter helps

obtain a stronger signal. Additionally, the data must be detrended in light of the excitation's asymmetrical shape.

4.3.2 Effect of Pole at Origin

To accurately identify the parameters of a flexible arm, it is crucial to address the interference caused by a pole at the origin introduced by the motor system. This pole can obscure the true characteristics of the flexible arm during system identification. In discrete systems, this pole occurs at $z = 1$. One effective strategy to mitigate this interference is to eliminate the pole at the origin before conducting the identification process.

The pole at the origin, essentially acting as an integrator, can be removed by differentiating the data before initiating the identification procedure. By doing so, the system's response is transformed, allowing for a clearer analysis of the flexible arm's behaviour without the influence of the integrative pole. After successfully identifying the parameters, reintroducing the pole at the origin is a straightforward process: the original data can be integrated again. This method ensures a more accurate and reliable identification of the flexible arm's parameters, since it is not obscured by the integrative interference, leading to a more precise understanding of the dynamics of the system.

4.3.3 Decision on Possible Orders of the Pole

In the realm of dynamic systems exhibiting oscillatory behaviors, simplifying the complexities in these systems often involves modelling them as combinations of springs. A spring model has a second-order response, typically. For the analysis of the system at hand, it is essential to account for the pole introduced by the integration effect of the DC motor, and additionally, at least one second-order model for the flexible bar. This basic consideration leads to a minimum requirement of a third-order system.

Upon closer observation of the system's response as shown in Figure (INSERT REFERENCE), a secondary oscillatory behavior becomes apparent, indicating the presence of multiple spring effects. Theoretically, the flexible bar could be represented by an infinite number of spring models. However, incorporating numerous second-order systems in series poses challenges such as overfitting and increased computational intensity during control. Hence, a reasonable approach is to limit the consideration to a maximum of a sixth-order system.

Several simulations were conducted using ten diverse input data, yielding results summarized in Table 3. The first and second columns detail the poles and the zeros configurations that minimize the error between model predictions and actual measurements for specific experimental data. The third column displays the corresponding errors for the best pole and zero that fits the data, while the last column reveals the variance across all errors derived from the poles and zeros under consideration. Data with significant error variance signifies sensitivity to different pole and zero combinations, which is probably more reliable. This is because a small variance between the errors indicates that changing the number of poles and zeros has little effect on the data.

Table 3: Experiment to Determine Model Order

Data ID	Pole	Zero	Error	Error Variance
1	3	2	0.0921	8.4675e-08
2	6	4	0.12511	2.1401e-06
3	5	1	0.048461	1.2950e-06
4	6	5	0.24045	1.3981e-06
5	5	2	0.18265	1.2368e-05
6	5	2	0.070397	1.0811e-05
7	5	3	0.60955	4.0704e-08
8	5	4	0.17042	1.8667e-05
9	4	3	0.12613	9.6481e-06
10	5	3	0.20494	4.3351e-04

Consequently, the model proposed by the tenth data batch was selected. Through this "search" analysis, we determined that an appropriate configuration for the system model to be five poles and three zeros. This aligns with our initial hypothesis of at least two spring effects (equivalent to four poles) and one DC motor integrator effect. Additionally, this method aided in determining an appropriate number of zeros.

4.4 ARMAX Model

ARMAX is a short form for the Auto-Regressive Moving Average model with eXogenuous inputs. It is a method that uses auto-regression to estimate the values of the model parameters from given data. The ARMAX function available on MATLAB is used to find a good estimate for the plant parameters. Hence, the model identification step was implemented using the ARMAX function.

The ARMAX function takes two input, an array (in the form: th = [the number of poles, number of zeros, the error dynamics, delay]) and the input signal, u. It outputs the numerator and the denominator of the transfer function of the plant.

The model identified using the ARMAX was simulated and the output is saved as $yf_{sim}(t)$. The result is compared with the measured value (which was differentiated), $yf(t)$. Root-mean-square error was used as a measure of deviation and to compare different models gotten from different data (as described in the previous subsection). The comparison plot for the "measured" data, $yf(t)$ and the simulated data $yf_{sim}(t)$ is given in Figure 5a.

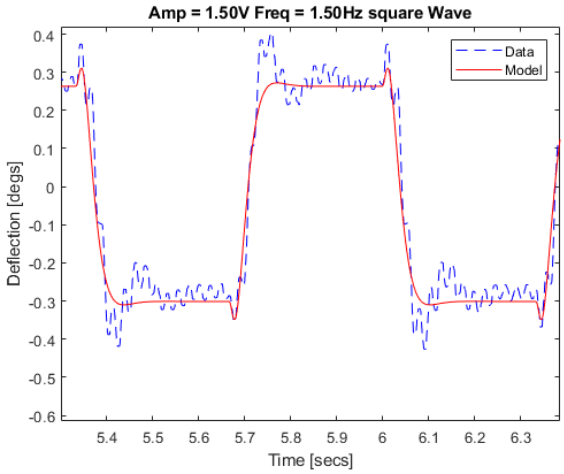

(a) The comparison plot between the "measured" data and the simulated data

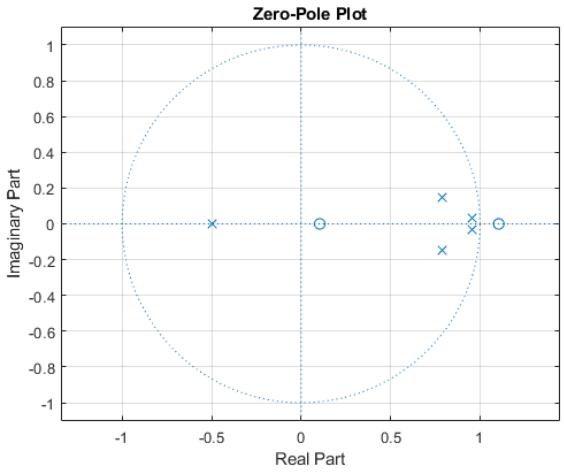

(b) Pole-zero diagram of the selected model

Figure 5: Plots relating to the "best" model identified

The transfer function of the model obtained from this identification process (prior to re-integrating) is given in the equation 1. This is the final ARMAX model. The poles and zeros are discussed in the next section (after the re-integration), however, the Figure 5b gives the positions of the poles and zeros the ARMAX identified model.

$$H(z) = \frac{-6.2415 \times 10^{-4} z^2 + 7.5421 \times 10^{-4} z - 7.1579 \times 10^{-5}}{z^5 - 2.9879 z^4 + 2.8306 z^3 - 0.3948 z^2 - 0.7394 z + 0.2918} \tag{1}$$

4.5 State-Space Model

After the completion of the model identification, the first step is to integrate the obtained model to determine the complete transfer function. We implemented this using the MATLAB *conv* function and we inspected the poles and zeros to ensure that it had functioned as expected. The eventual transfer function for the model is given as shown in Equation 2.

$$H(z) = \frac{-0.6242 \times 10^{-3} z^2 + 0.7542 \times 10^{-3} z - 0.0716 \times 10^{-3}}{z^6 - 3.9879 z^5 + 5.8186 z^4 - 3.2254 z^3 - 0.3447 z^2 + 1.0312 z - 0.2918} \tag{2}$$

The poles and zeros are provided in Equations below and the pole diagram is given in Figure 6. The dominant pole pairs causing the primary oscillation and the second observed pole pair can be seen in the figure. And it is very important that the poles are all within the unit circle which proves that the system is controllable.

$$
\begin{aligned}
Poles : & -0.4975 + 0.0000i \\
& 1.0000 + 0.0000i \\
& 0.9546 + 0.0324i \\
& 0.9546 - 0.0324i \\
& 0.7881 + 0.1477i \\
& 0.7881 - 0.1477i
\end{aligned}
$$

$$
\begin{aligned}
Zeros : & 1.1045 \\
& 0.1038
\end{aligned}
$$

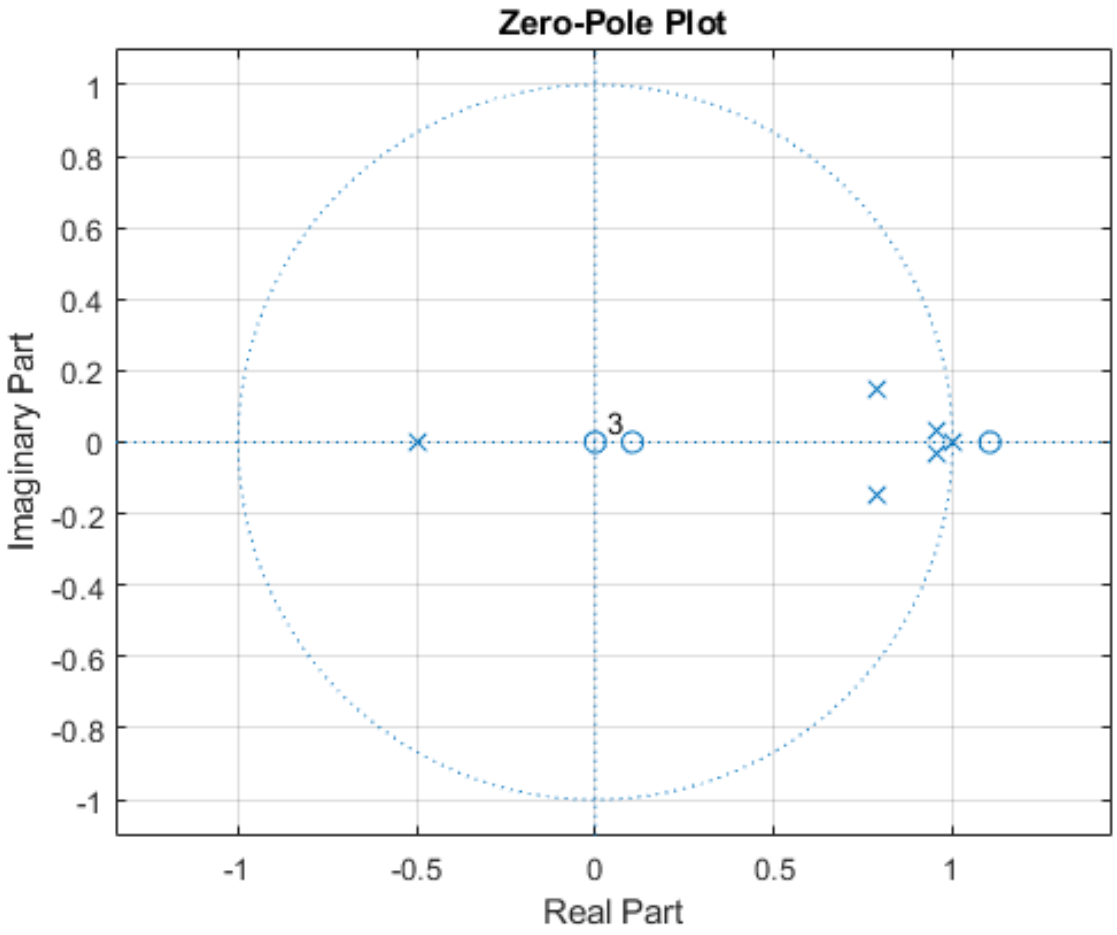

Figure 6: Poles and Zeros of Identified Model

$$A = \begin{bmatrix} 3.9879 & -5.8186 & 3.2254 & 0.3447 & -1.0312 & 0.2918 \\ 1.0000 & 0 & 0 & 0 & 0 & 0 \\ 0 & 1.0000 & 0 & 0 & 0 & 0 \\ 0 & 0 & 1.0000 & 0 & 0 & 0 \\ 0 & 0 & 0 & 1.0000 & 0 & 0 \\ 0 & 0 & 0 & 0 & 1.0000 & 0 \end{bmatrix}$$

$$B = \begin{bmatrix} 1 \\ 0 \\ 0 \\ 0 \\ 0 \\ 0 \end{bmatrix}$$

$$C = 1.0 \times 10^{-3} \times \begin{bmatrix} -0.6242 & 0.7542 & -0.0716 & 0 & 0 & 0 \end{bmatrix}$$

$$D = 0$$

Hence, the state space equation is:

$$\begin{aligned} x(k+1) &= Ax(k) + Bu(k) \\ y(k) &= Cx(k) + Du(k) \end{aligned}$$